Green Chemistry

COMMUNICATION

View Article Online
View Journal | View Issue

Cite this: *Green Chem.*, 2016, **18**, 406

Received 14th July 2015,
Accepted 7th August 2015

DOI: 10.1039/c5gc01600b

www.rsc.org/greenchem

Operando XAFS of supported Pd nanoparticles in flowing ethanol/water mixtures: implications for catalysis†

Mark A. Newton,*[a] John B. Brazier,[b] Elena M. Barreiro,[b] Stephen Parry,[c] Herman Emmerich,[d] Luis A. Adrio,[b] Christopher J. Mulligan,[b] Klaus Hellgardt*[e] and King Kuok (Mimi) Hii*[b]

Ethanol–water, a prototypical 'green' solvent mixture, cannot be considered as inert toward supported Pd nanoparticles. We establish severe size dependencies in Pd redox behavior, persistent gradients in Pd phase in a plug-flow situation, and that Pd nanoparticles are contaminated with hydrogen derived from the solvent.

Atom efficient catalysis and continuous flow methods are important enabling technologies for the manufacture of fine chemicals and pharmaceuticals, where the use of solvent is ubiquitous and counts as the single greatest contributor to overall environmental impact of these processes.[1–6] The choice of a solvent is primarily driven by physiochemical properties (polarity, protic or aprotic) that are compatible with the reactants, while rendering the appropriate environment required to deliver the optimal rate and selectivity. In recent years, there have been several monographs[6–11] produced by the pharmaceutical industry to assess and clarify the use of organic solvents. In all of these reviews, water and ethanol consistently scored very favourably by existing metrics.

Perhaps as a result of this, ethanol–water is used extensively in a myriad of Pd-catalyzed reactions, including redox processes[12] and all of the major cross-coupling reactions.[13–16] As such we have studied how supported palladium – starting from nanoparticulate PdO – behaves when exposed to mixtures of ethanol and water. Through time and spatially resolved Extended X-ray Absorption Fine Structure (EXAFS) we attempt to quantify and understand fundamental solvent-Pd interactions and how they influence the development and behaviour of the Pd as a function of its loading within the paradigm of a continuous plug flow reactor.

EXAFS provides a powerful means to directly address the oxidation states and structure of Pd *in operando* with high temporal and spatial resolution. There now exist a number of examples of this technique being applied to study various aspects of Pd catalyzed selective oxidation[17–22] and homogeneous[23–28] and heterogeneous[29,30] catalytic carbon–carbon coupling. However, these operando EXAFS studies have traditionally employed recirculating batch reactors. Here, our studies are performed using a continuous flow reactor,[30] which is industrially more relevant in terms of scale up and ease of operation; for this reason alone research into flow based processing solutions has expanded rapidly in recently years.[31–33] Within the context of the present study, a continuous flow arrangement can also provide both spatial and temporal windows into fundamental chemistry occurring within supported Pd system, making them easier to observe and quantify compared to a batch situation.

Using this method we demonstrate that when in contact with a mixture of ethanol and water Pd exhibits very large loading (particle size) dependencies in its redox behaviour that lead to persistent axial gradients in the structure of the metal phase. Moreover, even when metallic Pd is formed, the Pd nanoparticles are significantly contaminated with stored hydrogen. This hydrogen arises from reactive chemistry occurring between the catalyst and the solvent mixture. The desired situation, wherein the solvent for a catalytic process is an inert carrier of other reactive species, is never obtained in this prototypical case. The ramifications of these observations for the continued "greening" of such chemistry using supported Pd nanoparticles are discussed.

Fig. 1(A) shows the overall experimental approach with Fig. 1(B–D) showing examples of normalised Quick EXAFS

[a]*Department of Physics, University of Warwick, Gibbet Hill Road, Coventry, CV4 7AL, UK. E-mail: M.Newton.2@warwick.ac.uk*
[b]*Department of Chemistry, Imperial College London, South Kensington, London SW7 2AZ, UK. E-mail: mimi.hii@imperial.ac.uk*
[c]*Diamond Light Source, Didcot, Oxfordshire OX11 0QX, UK*
[d]*Swiss-Norwegian Beamline (SNBL) European Synchrotron Radiation Facility (ESRF), 6 rue Jules Horowitz, 38000 Grenoble, France*
[e]*Department of Chemical Engineering, Imperial College London, South Kensington, London SW7 2AZ, UK. E-mail: k.hellgardt@imperial.ac.uk*

†Electronic supplementary information (ESI) available: Catalyst synthesis, operando EXAFS measurements, linear combination analyses, transmission electron microscopy, comparison of 1, 2, and 5 wt% Pd systems. See DOI: 10.1039/c5gc01600b

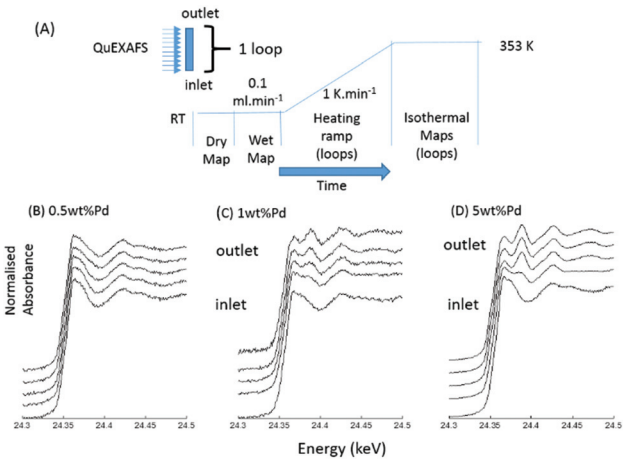

Fig. 1 (A) Experimental method (see also ESI†). Transmission QuEXAFS spectra are repeatedly collected at different axial positions along the catalyst bed whilst it is heated to, and then maintained at, 353 K under a flow (0.1 ml min^{-1}) of 50 : 50 EtOH/H_2O. (B–D) Representative and normalised Pd K-edge XAFS from different axial positions within catalyst beds comprised of (B) 0.5 wt% Pd/Al_2O_3; (C) 1 wt% Pd/Al_2O_3; and, (D) 5 wt% $PdAl_2O_3$.

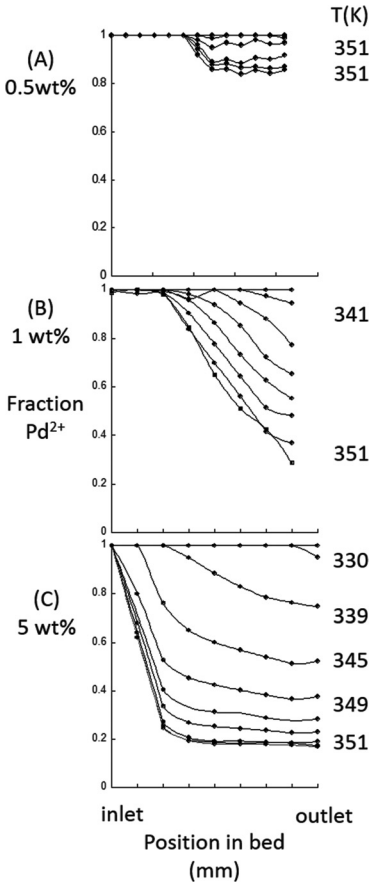

Fig. 2 Results of LCA analysis of the Pd K-edge XANES for the approximate fraction of Pd in the Pd^{2+} state as a function of time and temperature for the 0.5, 1, and 5 wt% Pd/Al_2O_3 cases shown in Fig. 1. The references used for the analysis were a Pd foil and bulk PdO powder.

(QuEXAFS) spectra obtained at the end of the experiment for supported Pd/γ-Al_2O_3 catalysts of 0.5, 1, and 5 wt% Pd loading.

Briefly, having established a flow of solvent through the catalyst bed transmission Pd K-edge Quick EXAFS measurements are made sequentially along the length of the bed to create maps of the chemicals state and structure of the Pd in the catalyst. This mapping process is continued as the sample is then heated to a maximal temperature of 353 K and continued for some time at this temperature (see also ESI†).

In their native form, all of the Pd catalysts contains significant amount of oxidised PdO, which undergoes reduction to Pd(0) by ethanol. What is interesting, and immediately evident from Fig. 1, is that neither the chemical state of the Pd in these systems, nor the manner in which it changes axially along the catalyst bed, is the same when the Pd loading is changed. The same experiment conducted using H_2O alone elicits no reduction of the PdO in any of the cases shown. As such the observed behaviour is ascribed to chemistry occurring ostensibly between the ethanol and the supported Pd.

By the end of our experiment hardly any of the Pd in the 0.5 wt% case appears to have changed from its native oxidised state. In stark contrast, at 5 wt%, Pd practically all of the catalyst bed has reduced to yield metallic Pd with oxidised Pd existing only at the reactor inlet. The 1 wt% case sits somewhere in between evidencing a more gradual shift from highly oxidised to predominantly reduced.

Fig. 2(a–c) shows, for the same three systems, results of a linear combination analysis (LCA) of the Pd K-edge XANES to assess the fractions of oxidised and reduced Pd present as a function of time, temperature, and position within the bed.

This analysis must be regarded as approximate as the references used are bulk metal foils and PdO. Nevertheless, it clearly shows the magnitude of the loading/size dependencies in the reduction process, and that a uniformly reduced catalyst bed is never attained. It also delineates from a spatial perspective how the reduction takes place, *i.e.* in the opposite direction of the flow from the reactor outlet to the inlet. This is commensurate with an earlier observation made during gas phase methane oxidation over Pt/Al_2O_3 catalysts at high temperature (603k),[34] and strongly indicative of cumulative reduction potential arising as the solvent passes along the bed in the direction of flow.

From the above it is clear that heating to 353 K under flowing EtOH/H_2O (50 : 50) can elicit the reduction of PdO to metallic Pd. It is also apparent that this is highly dependent on the average size of the Pd nanoparticles (see also ESI†) and that, within an environment under continuous flow of an alcoholic solvent, persistent Pd-phase gradients develop backwards from the reactor exit toward the inlet.

Fig. 3 shows the results of analysing the EXAFS obtained during these experiments for 1, 5, and 10 wt% systems.

Fig. 3(A) reports the first shell coordination numbers pertaining to any fcc, metallic Pd phase (N_1^{Pd}) as a function of time/temperature, for 10 wt% (open circles) and 5 wt% systems (filled circles), whilst Fig. 3(B) reports the first shell PdPd bondlengths (R_1^{Pd}) returned for these samples along with those derived for a Pd foil (crosses) used as an internal reference. Fig. 3 (C) and (D) show the same data for a 1 wt% Pd system.

EXAFS analysis yields more information as to the development of the reduced Pd phase. Firstly, the onset of PdO reduction, and formation of fcc Pd nanoparticles, occur at lowest temperature in the 10% case and the highest in the 1 wt%.

Secondly, the inlet of the bed remains to varying degrees oxidised in each case, with the 1 wt% showing no evidence of reduced Pd at the reactor inlet throughout the experiment. Fig. 3 also shows that the 1 wt% case, as might be expected, eventually yields Pd particles that are very much smaller than observed in the 5 and 10 wt% cases.[35] The latter pair, within the error associated with this measurement, appear very similar in terms of the size of the average Pd nanoparticle implied to be formed by the end of the experiment.

When reduced 5 and 10 wt% Pd catalysts show values of R_1^{Pd} that are consistently larger than those obtained from the Pd reference foils. Previous work[36] has established that clean Pd nanoparticles of the size implied from the values of N_1^{Pd} (and TEM, see ESI†) should never show PdPd bond lengths longer than found in a foil. In the 1 wt% case, when maximally reduced toward the outlet of the reactor, average values of *ca.* 2.73–2.74 Å are indicated. Although these might also be considered large for the size of the Pd particles within this sample, it is much less easy to establish whether they are equally anomalous.

In the case of Pd,[36] and in the absence of other factors, smaller particle sizes are accompanied by smaller bond distances. As such, the expanded bond lengths in the 5 and 10 wt % cases result from the process of reduction of the Pd by the solvent. There are two possible explanations for this: first, adsorbates may form and bind to the surfaces of the nanoparticles lengthening the surface PdPd bonds to such a degree that the average bonding within the particle, as observed by the EXAFS, appears extended; or, the Pd nanoparticles may have expanded as a result of incorporation of another element. The ability for Pd to absorb atomic hydrogen (to form Pd H_x phases) or carbon (to yield PdC_x) is well established,[37–43] and both of these interstitial compounds are known to be thermally stable at the temperatures we have applied.

Fig. 4 shows the results obtained from a further experiment. In this case (black) the 1 wt% Pd system was maintained at

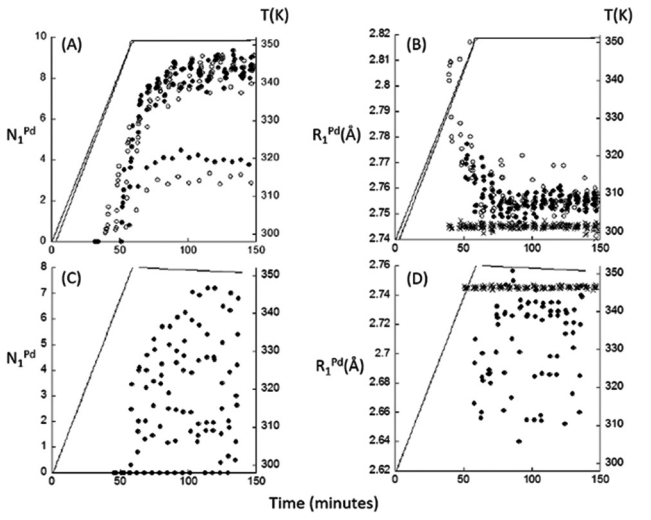

Fig. 3 (A) and (B) Comparison of the behaviour of 5 (filled circles) and 10 (open circles) wt% Pd/Al_2O_3 catalysts during heating under flowing $EtOH/H_2O$ (50 : 50) from analysis of the Pd K-edge EXAFS. (A) 1st shell, fcc Pd coordination number (N_1^{Pd}) and (B) 1st shell PdPd bond length (R_1^{Pd}). In each panel the solid black lines show the heating ramps (right hand abscissa). Panels (C) and (D) report the same parameters but for a 1 wt% Pd/Al_2O_3 sample. In panels (B) and (D) the crosses are the R_1^{Pd} values returned from analysis of the reference Pd foil (B). These plots contains all data obtained for each loop and each axial position, from inlet to outlet, in the bed and therefore also reflect the axial gradients in structure of the Pd phase as they develop.

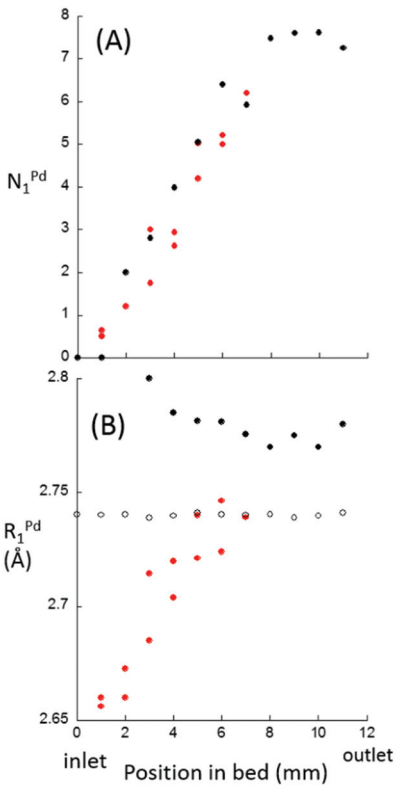

Fig. 4 Comparison of N_1^{Pd} (A) and R_1^{Pd} (B) as a function of axial position along the reactor bed for 1 wt% Pd/Al_2O_3 heated under flowing $EtOH/H_2O$ and maintained at 353 K under the flowing solvent for *ca.* 1.5 hours (red) and 11 hours (black). In Fig. 3(B) the open circles report R_1^{Pd} obtained from the reference Pd foil. The sample run for 1.5 hours was under constant X-ray illumination. The 11 hour experiment was run in the absence of X-rays and only exposed post reaction for the duration of the mapping process (*ca.* 15 minutes) at 298 K.

353 K under flowing EtOH/H_2O for 11 hours before the system was exposed to X-rays for mapping of the catalyst bed at room temperature. The results of EXAFS analysis of this mapped bed are compared to those derived from the very end (last two loops) of the experiment already described (Fig. 1 and 2, *ca.* 1.5 hours at 353 K in the X-ray beam-red). Fig. 4(A) reports the axial variation in N_1^{Pd} in the two cases, Fig. 4(B) the corresponding variations in R_1^{Pd}. Again the result of the fitting the Pd reference foil are also given (open circles) in Fig. 4(B).

Fig. 4(A) reveals that the results for N_1^{Pd} are practically identical. In the 1 wt% case, the evolution of the catalyst bed appears to become stuck; the axial gradients in reduced Pd seen after 1.5 hours (see Fig. 2) remain the same even after a further 10 hours of operation. The values of R_1^{Pd} (Fig. 4(B)) obtained after 1.5 or 11 hours of flow operation show a marked difference. After 11 hours the PdPd bond length has increased significantly (ranging from 2.8 to 2.77 Å) and the axial gradient in R_1^{Pd} has flattened.

These experiments demonstrate that the chemistry being observed is not due to the X-rays themselves. Furthermore, these latter observations establish the extended PdPd bonding as the result of a storage of atomic hydrogen; it is only by the formation of such PdH_x phases that such extended PdPd bonding within can be reasonably explained.

The differences in R_1^{Pd} values shown in Fig. 4(B) and the time/temperature dependence of the R_1^{Pd} curves for the 5 and 10% Pd systems (Fig. 3) can now also be understood as reflecting the thermal stability of the PdH_x phase and the establishment of the following equilibrium in these systems from the very earliest stages of Pd reduction:

$$Pd^0 + 0.5\ xH_2 \leftrightarrow PdH_x \quad (1)$$

In the 5 and 10 wt% cases it appears that the Pd nanoparticles initially formed are heavily contaminated with hydrogen. Over similar Pd/Al_2O_3 and Pd/C catalysts, using EXAFS as a probe, McCaulley[38] established that a PdH_x (x = 0.44) phase has R_1^{Pd} bond lengths of 2.81–2.82 Å, which (from Fig. 3) are also attained in the very earliest stages of the reduction of the 10 wt% Pd sample. As the temperature of the sample is increased equilibrium [1] gradually shifts to the left, as demonstrated by Fig. 3, but never to the point where the reduced Pd nanoparticles can be considered free from hydrogen contamination.

Our experiments therefore reveal and quantify two separate consequences of exposing supported Pd, starting with nanoparticulate PdO, to a prototypical green solvent mixture.

The results reveal large differences in redox behaviour over the range of Pd content investigated. For a 0.5 wt% Pd catalyst (Fig. 1 and 2), no evidence was found for the formation of a discrete metallic phase. This contrasts with the relatively facile reduction of Pd that occurs at loadings of ≥5 wt%. However, even at these loadings, a small proportion of the bed at the reactor inlet remains significantly oxidised. A homogeneous axial Pd phase distribution is therefore never achieved and, in the limit of high Pd dispersion, severe gradients in oxidic/metallic Pd arise that are extremely persistent.

We envisage that the initial reduction of PdO by ethanol can occur primarily in two ways as shown in Scheme 1; we have previously suggested[30] that the second route (b) is more likely, as it could result in a cumulative reduction potential along the bed in the direction of the flow and thus lead to the types of steady state gradients observed.

Analysis of the EXAFS (rather than simple mapping from XANES[30]) shows that this scheme needs to be augmented to take account of an initial high level of hydrogen storage. In addition Pd nanoparticles will themselves be able to catalyse reduction of ethanol further feeding further feed into equilibrium [1] to accelerate downstream reduction of more Pd.

Investigations with a 2 wt% catalyst (see ESI†) show its behaviour is more akin to that displayed by the 1 wt% Pd case than the 5 wt%. This suggests that the redox properties of supported Pd display a step change as a function of particle size (between *ca.* 3–4 nm, see ESI†). This change in behaviour is the foundation for the observed differences between these catalysts.

Evidence for size-dependent changes in the properties of Pd has been previously obtained from *ex situ* XPS measurements of Pd/C catalysts used in aerobic oxidation of glucose.[44] The redox behaviour of Pd nanoparticles in high temperature CO oxidation[45] has also been observed to change abruptly between a Pd loading of 4 wt% (*ca*. 4 nm average particle diameter) and 2 wt% (*ca*. 3 nm average particle diameter). Given the very different experimental conditions involved in these and the current case, it would seem that switching of the chemical properties of Pd nanoparticles occurs somewhere between *ca.* 3 and 4 nm, which has important implications for their catalytic applications. The fundamental behaviour we have observed of supported Pd interacting with an EtOH/H_2O solvent also has further ramifications for the adoption of this system on a large scale. Firstly, the induction of phase gradients under flow must be considered as deleterious to any applied process situation. Secondly, reducing the loading of Pd may not result in the desired atom efficiency one might expect. Our results show that below *ca.* 3 nm particle size the supported Pd will have a strongly enhanced tendency to remain oxidised which may or may not be appropriate for the desired process chemistry.

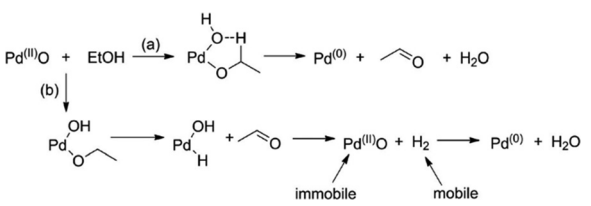

Scheme 1 Two possible routes for ethanol to reduce PdO and form Pd nanoparticles which may further oxidise solvent molecules and/or store and release H subsequently eliciting further Pd reduction downstream.

Further, the contamination of Pd nanoparticles by hydrogen may have a number of consequences: theoretical studies have shown that subsurface H in Pd nanoparticles may significantly affect the stability of adsorbates on the surfaces on these particles;[46] particle morphologies, and therefore the number and type of potential reactive sites, themselves may also be altered as a result of such bulk contamination. As such the formation of PdH_x, rather than clean Pd, may have profound effects in directing the overall catalytic properties of the system.

Equilibrium [1] demonstrates that PdH_x should be removable from such systems through operation at higher temperatures. However, this may also promote undesirable leaching of Pd.[29,47] Within the development of green processes this solution may also be regarded as self-defeating as it requires a greater energy input and thus lower overall process efficiency.

In summary, the use of a prototypical green solvent mixture of a primary alcohol and water has a number of reactive ramifications for supported Pd nanoparticles that must be understood before one may start to consider the suitability of such systems for catalysis. These are: extreme changes in the basic redox behaviour of the Pd as a function of particle size resulting in persistent and undesirable gradients in Pd structure within a flow reactor; and, extensive formation of PdH_x. Whilst some of these factors could be avoided through higher temperature and pressure operation this may not be desirable for the overall process efficiency. At least in the case of supported Pd, it seems clear that more basic research into understand how such differing factors may be controlled may provide the best long term route for the attainment of greener process solutions for fine chemical synthesis.

Acknowledgements

The work was funded by the EPSRC (UK) research grant: "Elucidate and Separate (ELSEP) – Palladium Catalysts in C–C and C–N Coupling Reactions" (grant number: EP/G070172/1). EMB was supported by Xunta Galicia, and CJM is supported by an industrial Doctoral Training Grant (AstraZeneca). The Diamond light source (UK) and the Swiss Norwegian Beamline at the ESRF (France) are gratefully acknowledged for access to facilities. We thank Johnson Matthey plc for the provision of Pd salts through an academic loan scheme and Dr Ana Iglesias-Juez and Prof. Marcos Fernandez-Garcia for their advice regarding the preparation of the catalysts used in this work. Ekaterina Wade (Imperial College) is gratefully acknowledge for assistance with the TEM measurements. MAN is extremely grateful to the Department of Physics, University of Warwick, United Kingdom or a visiting academic position.

Notes and references

1 R. A. Sheldon, *Pure Appl. Chem.*, 2000, **72**, 1233.
2 D. M. Roberge, B. Zimmermann, F. Rainone, M. Gottsponer, M. Eyholzer and N. Kockmann, *Org. Process Res. Dev.*, 2008, **12**, 905.
3 P. J. Dunn, K. K. Hii, M. J. Krische and M. T. Williams, Sustainable Catalysis: Challenges and Practices for the Pharmaceutical and Fine Chemical Industries, in *Green Chemistry in the Pharmaceutical Industry*, ed. P. J. Dunn, K. K. Hii, M. J. Krische and M. T. Williams, Wiley, NY, 2013.
4 R. A. Sheldon, *Chem. Soc. Rev.*, 2012, **41**, 1437.
5 J. Wegner, S. Ceylan and A. Kirschning, *Adv. Synth. Catal.*, 2012, **354**, 17.
6 C. Capello, U. Fischer and K. Hungerbühler, *Green Chem.*, 2007, **9**, 927.
7 R. K. Henderson, C. Jimenez-Gonzalez, D. J. C. Constable, S. R. Alston, G. G. A. Inglis, G. Fisher, J. Sherwood, S. P. Binks and A. D. Curzons, *Green Chem.*, 2011, **13**, 854.
8 V. V. Ranade, M. K. Sharma, A. A. Kulkarni and D. J. Ager, *Synthesis*, 2015, 760.
9 D. Prat, J. Hayler and A. Wells, *Green Chem.*, 2014, **16**, 4546.
10 P. J. Dunn, *Chem. Soc. Rev.*, 2012, **41**, 1452.
11 K. Alfonis, J. Colberg, P. J. Dunn, T. Fevig, S. Jennings, T. A. Johnson, H. P. Kleine, C. Knight, M. A. Nagy, D. A. Perry and M. Stefaniak, *Green Chem.*, 2008, **10**, 31.
12 Hydrogenation: P. D'Arrigo, G. Pedrocchi-Fantoni and S. Servi, *Tetrahedron: Asymmetry*, 2010, **21**, 914; S. Gunzenhauser, E. Biala and P. Strazewski, *Tetrahedron Lett.*, 1998, **39**, 6277; M. R. Wiley, L. C. Weir, S. Briggs, N. A. Bryan, J. Buben, C. Campbell, N. Y. Chirgadze, R. C. Conrad, T. J. Craft, J. V. Ficorilli, J. B. Franciskovich, L. L. Froelich, D. S. Gifford-Moore, T. Goodson Jr., D. K. Herron, V. J. Klimkowski, K. D. Kurz, J. A. Kyle, J. J. Masters, A. M. Ratz, G. Milot, R. T. Shuman, T. Smith, G. F. Smith, A. L. Tebbe, J. M. Tinsley, R. D. Towner, A. Wilson and Y. K. Yee, *J. Med. Chem.*, 2000, **43**, 883.
13 Oxidation of alcohols: Y. Ito, H. Ohta, Y. M. A. Yamada, Y. Uozumi and T. Enoki, *Tetrahedron*, 2014, **70**, 6146; G. An, H. Ahn, K. A. De Castro and H. Rhee, *Synthesis*, 2010, 477.
14 Suzuki–Miyaura: Q. Du and L. Yiqun, *Beilstein J. Org. Chem.*, 2011, **7**, 378; F. Amorosoa, S. Colussia, A. Del Zottoa, J. Llorcab and A. Trovarellia, *Catal. Commun.*, 2011, **12**, 563.
15 Sonogashira coupling: C. Duplais, A. J. Forman, B. A. Baker and B. H. Lipshutz, *Chem. – Eur. J.*, 2010, **16**, 3366.
16 Heck reaction: Y.-Q. Yuan and S.-R. Guo, *Synth. Commun.*, 2012, **42**, 1059; M. Hosseini-Sarvari, Z. Razmi and M. M. Doroodmand, *Appl. Catal., A*, 2014, **475**, 477.
17 J. D. Grunwaldt, M. Caravati and A. Baiker, *J. Phys. Chem. B*, 2006, **110**, 25586.
18 A. F. Lee and K. Wilson, *Green Chem.*, 2004, **6**, 37.
19 A. F. Lee, S. F. Hackett, J. S. J. Hargreaves and K. Wilson, *Green Chem.*, 2006, **8**, 549.
20 S. F. J. Hackett, R. K. Brydson, M. H. Gass, I. Harvey, A. D. Newman, K. Wilson and A. F. Lee, *Angew. Chem., Int. Ed.*, 2007, **46**, 8593.

21 A. F. Lee, C. V. Ellis, J. N. Naughton, M. A. Newton, C. M. A. Partlett and K. Wilson, *J. Am. Chem. Soc.*, 2011, **133**, 5724.
22 C. M. A. Partlett, C. V. Gaskell, J. N. Naughton, M. A. Newton, K. Wilson and A. F. Lee, *Catal. Today*, 2013, **205**, 76.
23 S. G. Fiddy, J. Evans, M. A. Newton, T. Neisius, R. P. Tooze and R. Oldman, *Chem. Commun.*, 2003, 2682.
24 J. Evans, L. O'Neill, V. L. Kambhampati, G. Rayner, S. Turin, A. Genge, A. J. Dent and T. Neisius, *J. Chem. Soc., Dalton Trans.*, 2002, 2207.
25 G. Guilera, M. A. Newton, C. Polli, M. Guino, S. Pascarelli and K. K. Hii, *Chem. Commun.*, 2006, 4306.
26 S. G. Fiddy, J. Evans, T. Neisius, M. A. Newton, T. Tsoureas, A. A. D. Tulloch and A. Danopoulos, *Chem. – Eur. J.*, 2007, **13**, 3652.
27 P. J. Ellis, I. S. Fairlamb, S. F. J. Hackett, K. Wilson and A. F. Lee, *Angew. Chem., Int. Ed.*, 2010, **49**, 1820.
28 L. A. Adrio, B. N. Nguyen, G. Guilera, A. G. Livingston and K. K. Hii, *Catal. Sci. Technol.*, 2012, **2**, 2578.
29 S. Reimann, J. Stötzel, R. Frahm, W. Kleist, J. D. Grunwaldt and A. Baiker, *J. Am. Chem. Soc.*, 2011, **133**, 3921.
30 J. B. Brazier, B. N. Nguyen, L. A. Adrio, E. M. Barreiro, W. P. Leong, M. A. Newton, S. J. A. Figueroa, K. Hellgardt and K. K. Hii, *Catal. Today*, 2014, **229**, 95.
31 R. L. Hartman, J. P. McMullen and K. F. Jensen, *Angew. Chem., Int. Ed.*, 2011, **50**, 7502.
32 S. V. Ley, *Chem. Rec.*, 2012, **12**, 378.
33 S. G. Newman and K. F. Jensen, *Green Chem.*, 2013, **15**, 1456.
34 J. Stöetzel, R. Frahm, B. Kimmerle, M. Nachtegaal and J. D. Grunwaldt, *J. Phys. Chem. C*, 2012, **116**, 599.
35 The value of N_1^{Pd} can be related to the number of atoms comprising the average nanoparticle. See for instance: (*a*) R. E. Benfield, *J. Chem. Soc., Faraday Trans.*, 1992, **88**, 1107; (*b*) A. Jentys, *Phys. Chem. Chem. Phys.*, 1999, **1**, 4059. However, this is approximate, as N_1^{Pd} may be subject to modification by other effects such as disorder. In the current case this will mean that within this approximation N_1^{Pd} will underestimate that actual average particle size. (see also ref. 38 for specific example of how this affects apparent coordination numbers for Al_2O_3 supported PdH_x *versus*, Pd nanoparticles).
36 Ordinarily, and isothermally, increasing Pd nanoparticle size should be accompanied by decreased disorder and a convergence (at *ca.* 4–5 nm diameter) of 1st Shell Pd–Pd bond distance with that of a bulk Pd foil *i.e.* 2.75 Å. See for instance: S. A. Nepjiko, M. Klimenkov, M. Adelt, H. Kuhlenbeck, R. Schlögl and H. J. Freund, *Langmuir*, 1999, **15**, 5309.
37 R. J. Davis, S. M. Landry, J. A. Horsely and M. Boudart, *Phys. Rev. B: Condens. Matter*, 1989, **39**, 10580.
38 J. A. McCaulley, *J. Phys. Chem.*, 1993, **97**, 10372.
39 J. A. McCaulley, *Phys. Rev. B: Condens. Matter*, 1993, **47**, 4872.
40 A. Rose, S. Maniguet, R. J. Mathew, C. Slater, J. Yao and A. E. Russell, *Phys. Chem. Chem. Phys.*, 2003, **5**, 3220.
41 H. Kobayashi, M. Yamauchi, H. Kitagawa, T. Kubota, K. Kato and M. Takata, *J. Am. Chem. Soc.*, 2008, **130**, 1828.
42 D. Teschner, J. Borsodi, A. Wootsch, Z. Revay, M. Havecker, A. Knop-Gericke, S. D. Jackson and R. Schlögl, *Science*, 2008, **320**, 86.
43 M. W. Tew, M. Naachtegaal, M. Janousch, T. Huthwelker and J. A. van Bokhoven, *Phys. Chem. Chem. Phys.*, 2012, **14**, 5761.
44 I. V. Delidovich, O. P. Taran, L. G. Matvienko, A. N. Simonov, I. L. Simakova, A. N. Bobrovskaya and V. N. Parmon, *Catal. Lett.*, 2010, **140**, 14.
45 A. Iglesias-Juez, A. Kubacka, M. Fernandez-Garcia, M. Di Michiel and M. A. Newton, *J. Am. Chem. Soc.*, 2011, **133**, 4484.
46 S. M. Kozlov, A. Hristiyan and K. M. Neyman, *J. Phys. Chem. C*, 2014, **118**, 15242.
47 See for a thorough review, D. Cantillo and O. Kappe, *ChemCatChem*, 2014, **6**, 3286.